Published by
NIGERIAN SOCIETY OF PHYSICAL SCIENCES
Available online @ https://journal.nsps.org.ng/index.php/jnsps

J. Nig. Soc. Phys. Sci. 7 (2025) 2795

Journal of the Nigerian Society of Physical Sciences

A robust deep learning approach for photovoltaic power forecasting based on feature selection and variational mode decomposition

Mokhtar Ali[a], Abdelkerim Souahlia[a], Abdelhalim Rabehi[a], Mawloud Guermoui[a,b], Ali Teta[c], Imad Eddine Tibermacine[d], Abdelaziz Rabehi[a], Mohamed Benghanem[e,*]

[a]*Laboratory of Telecommunication and Smart Systems (LTSS), Faculty of Science and Technology, University of Djelfa, PO Box 3117, Djelfa 17000, Algeria*
[b]*Unité de Recherche Appliquée en Energies Renouvelables, URAER, Centre de Développement des Energies Renouvelables, CDER, 47133, Ghardaïa, Algeria*
[c]*Applied Automation and Industrial Diagnostics Laboratory (LAADI), Faculty of Sciences and Technology, University of Djelfa, 17000 DZ, Algeria*
[d]*Department of Computer, Control, and Management Engineering, Sapienza University of Rome, 00185, Rome, Italy*
[e]*Physics Department, Faculty of Science, Islamic University of Madinah, Madinah, 42351, Saudi Arabia*

Abstract

Accurate forecasting of photovoltaic (PV) power is essential for effective grid integration and energy management, particularly in solar-rich regions such as Algeria. This study presents a robust forecasting framework that combines advanced feature selection techniques with deep learning architectures—namely MLP, GRU, LSTM, BiLSTM, and CNN—to enhance daily PV power prediction accuracy. Three feature selection methods—ReliefF, Minimum Correlation, and Minimum Redundancy Maximum Relevance (MRMR)—are employed to identify the most relevant input variables from a dataset collected in the Ghardaïa region. Among the selected predictors, Global Solar Radiation (GSR) consistently proves to be the most influential. To further enhance model inputs, Variational Mode Decomposition (VMD) is applied to extract informative Intrinsic Mode Functions (IMFs) from the selected features. A comparative evaluation of the models indicates that recurrent neural networks, particularly GRU and LSTM, deliver superior performance across various metrics, including RMSE, MAE, nRMSE, nMAE, R^2, and the correlation coefficient. The GRU model achieves the best results, with an RMSE of 3.246 and an R^2 of 0.9550 using five IMFs. These findings highlight the effectiveness of integrating optimal feature selection, signal decomposition, and deep learning for reliable PV power forecasting. The proposed hybrid approach provides a practical and scalable solution for enhancing energy planning and operational efficiency in high-solar-potential regions.

DOI:10.46481/jnsps.2025.2795

Keywords: PV power, Renewable energy, Feature selection, Artificial Neural Networks, Forecasting.

Article History :
Received: 23 March 2025
Received in revised form: 18 April 2025
Accepted for publication: 06 May 2025
Available online: 26 May 2025

Communicated by: B. J. Falaye

1. Introduction

As the world confronts the dual challenges of climate change and the rapid depletion of fossil fuel reserves, the transition to renewable energy has become a critical global imperative [1]. Among the various renewable energy sources, solar

*Corresponding author Tel. No.: +966-50-734-6783.
Email address: mbenghanem@iu.edu.sa (Mohamed Benghanem)

energy stands out due to its cleanliness, abundance, and sustainability. Solar technologies harness the sun's energy to produce light, heat, and electricity, serving both residential and industrial needs.

The continued extraction and consumption of conventional energy resources—such as coal, oil, and natural gas—not only accelerate their depletion but also contribute significantly to environmental degradation. These realities underscore the urgency of adopting cleaner energy alternatives. Solar energy, in particular, offers immense potential with minimal ecological impact.

Driven by international efforts to reduce carbon dioxide (CO2) emissions [2, 3], the demand for renewable electricity is steadily rising. Photovoltaic (PV) technology is emerging as one of the most promising renewable energy solutions for both developed and developing nations. Its advantages are numerous: it is environmentally friendly—producing electricity without releasing greenhouse gases like CO2 and nitrogen oxides (NO?); economically beneficial—reducing energy costs and fostering job creation; and well-suited for decentralized energy production, especially in remote or underserved regions.

The electricity generation capacity of PV systems is highly dependent on their geographical location, specifically on local solar irradiation levels. As illustrated in Figure 1 [4]. solar energy exhibits significant production potential worldwide. However, the efficiency of most commercially available solar cells remains within 10% to 20% [5]. Despite recent technological advancements, this limited efficiency suggests considerable room for improvement.

The efficiency of PV systems is closely tied to the geographic and climatic conditions of their deployment. Algeria, for instance, possesses one of the highest solar energy potentials in the world, with annual sunshine ranging from 2,000 to 3,900 hours and daily solar irradiation between 3,000 and 6,000 Wh/m² [6]. Despite this exceptional potential, the efficiency of commercially available solar cells typically falls between 10% and 20%, highlighting the need for ongoing advancements in materials, design, and system optimization [7–10].

A key challenge in integrating solar power into electrical grids is the variability and intermittency of solar radiation. To maintain grid reliability and ensure efficient energy planning, the development of accurate forecasting models and energy storage systems is essential. Forecasting techniques are often categorized by time horizons: medium-term (days ahead), short-term (hours ahead), and very short-term (minutes ahead), each serving distinct purposes in energy management, grid operation, and real-time decision-making [11].

In this context, artificial intelligence (AI) has emerged as a powerful tool for solar forecasting. AI techniques are particularly adept at handling the nonlinear, dynamic, and often noisy nature of solar energy data. Methods such as artificial neural networks (ANN), support vector machines (SVM), decision trees, and advanced deep learning models—including convolutional neural networks (CNN) and long short-term memory (LSTM) networks—have demonstrated significant promise in improving forecast accuracy across various time scales.

Forecasting methods can generally be classified into four main categories: physical, statistical, artificial intelligence (AI)-based, and hybrid approaches. Hybrid forecasting methods combine elements of the three aforementioned techniques to leverage their respective strengths and improve overall predictive performance Wan *et al*. [12].

To provide a clearer understanding of the core characteristics of each method, a series of comparative tables is presented. Table 1 provides an overview of physical forecasting methods, which rely heavily on meteorological data and physical modeling principles. Table 2 focuses on statistical techniques that utilize historical data and regression-based approaches. Table 3 outlines AI-based prediction methods, emphasizing machine learning algorithms that enhance forecasting performance.

A number of reviews have emphasized the rapid growth and evolution of forecasting methodologies. Antonanzas *et al*. [13], for example, provided a comprehensive classification of forecasting approaches by time horizon, input type, and application. Similarly, Van der Meer *et al*. [14] underscored the growing importance of probabilistic forecasting in managing uncertainty and enhancing grid resilience.

Overall, Table 4 offers a valuable overview of contemporary research trends, serving as a reference for selecting suitable forecasting strategies tailored to specific regional and operational needs.

Selecting suitable predictors for accurate PV power forecasting is both challenging and time-consuming. The arbitrary choice of input features often leads to redundancy and strong intercorrelations, which increase the input space and model complexity—ultimately reducing forecasting accuracy. This study aims to identify the most relevant predictors that minimize model complexity while maximizing forecasting performance. To achieve this, we apply several feature selection methods including ReliefF, Minimum correlation technique, and Minimum Redundancy Maximum Relevance technique MRMR to evaluate the importance of commonly used variables. The selected optimal features are then used as inputs to an Artificial Neural Network (ANN) model for PV power forecasting.

Our approach is validated using a real-world dataset collected from the Ghardaïa region in Algeria, covering the period from 2018 to 2019. The model's performance is evaluated using multiple objective metrics. Each input variable is ranked according to its contribution to the forecast, and the top-ranking features are then used to train various models, including Multi-Layer Perceptron (MLP), Gated Recurrent Unit (GRU), Long Short-Term Memory (LSTM), Bidirectional LSTM (BiLSTM), and Convolutional Neural Network (CNN), for PV power prediction.

The remainder of this paper is structured as follows: Section 2 introduces the PV plant and data used in the study. Section 3 presents the theoretical foundations and the proposed methodology. Section 4 describes the experimental design, including data preprocessing, model development, and evaluation procedures. Section 5 discusses the results and performance analysis. Finally, Section 6 summarizes the conclusions and suggests potential directions for future research.

2. Overview of the solar photovoltaic plant

To validate the forecasting models, this study focuses on a photovoltaic power plant located in the Ghardaïa region of Algeria. The facility, operated by *SKTM*, is situated about 15 kilometers north of Ghardaïa city, near the village of Oued Nechou. The site lies in a semi-desert environment, with geographical coordinates of 32°35′59″N 3°42′16″E at an altitude of 566 meters. Figure 2 illustrates the plant's location on the map of Algeria.

Oued Nechou benefits from intense solar radiation, ranging between 900 and 1000 W/m² during summer months, typical of Saharan climates known for extreme heat and frequent sandstorms. The plant functions as a pilot site designed to evaluate the performance of photovoltaic technologies under local environmental conditions. Its installed capacity is around 1100 kWc.

Established in 2014 as part of Algeria's National Renewable Energy Program, this plant was one of the earliest PV facilities developed before the construction of 23 additional plants across the country's high plateau and southern zones. Together, these projects aim to contribute 400 megawatts to the national energy grid. The Ghardaïa plant incorporates various PV technologies, including thin-film amorphous silicon (a-Si), cadmium telluride (Cd-Te), polycrystalline silicon, and monocrystalline silicon (a-Si/n-type a-Si).

3. Theory

In this section, we present the theoretical background relevant to the key aspects addressed in this study. We explore the domain of feature selection techniques and discuss the forecasting models employed, namely the Multi-Layer Perceptron (MLP), Gated Recurrent Units (GRU), Long Short-Term Memory (LSTM), Bidirectional LSTM (BiLSTM), and Convolutional Neural Network (CNN).

3.1. Features selection

In typical forecasting scenarios, datasets for predicting PV power include multiple predictors, such as temperature (T), number of day (nD), number of hour (nH), and global solar radiation (GSR), among others. Due to this abundance of features, feature selection plays a critical role in identifying the most relevant predictors for building an effective predictive model. These techniques evaluate the importance of each predictor—referred to as an input parameter—in relation to its contribution to forecasting the output.

As outlined previously, the primary aim of this study is to determine the optimal combination of input parameters that enable accurate PV power prediction. To achieve this, three feature selection techniques have been utilized. These methods help reduce data dimensionality, eliminate redundancy and noise, decrease model complexity, and ultimately enhance predictive performance.

3.1.1. ReliefF technique

The ReliefF algorithm, proposed by Kira and Rendell in 1992 [15, 16], is a robust technique utilized in ML and data mining to identify relevant features for classification tasks. It systematically evaluates the discriminatory power of each feature by analyzing the differences in feature values between instances of the same and different classes [17].

During each iteration of the algorithm, the weight (W_i) assigned to each feature (i) is updated based on the observed differences. This update is governed by the following equation:

$$W_i = W_i - (x_i - nearHIT_i)^2 + (x_i - nearMISS_i)^2 \quad (1)$$

where W_i is the weight for feature I, x_i is the value of feature i for the current instance, $nearHIT_i$ and $nearMISS_i$ are the corresponding feature values of the nearest neighbors from the same and different classes, respectively.

ReliefF iteratively updates feature weights, assigning greater weight to features that better differentiate between classes. One of its key strengths is its ability to handle both categorical and continuous features, and its computational efficiency makes it suitable for high-dimensional datasets.

3.1.2. Minimum correlation technique

The Minimum CFS method is a straightforward yet effective approach for feature selection. It identifies the most relevant features by analyzing the correlation matrix C, where each element $C_{i,j}$ represents the correlation between features $f_i$and f_j.

The correlation matrix C is:

$$C = \begin{bmatrix} C_{1,1} & C_{1,2} & \dots & C_{1,p} \\ C_{2,1} & C_{2,2} & \dots & C_{2,p} \\ \vdots & \vdots & \ddots & \vdots \\ C_{p,1} & C_{p,2} & \dots & C_{p,p} \end{bmatrix}. \quad (2)$$

The weight W_i of feature f_i is computed as the average correlation with all other features:

$$W_i = score_i = \frac{1}{p}\sum_{j=1}^{p} C_{i,j}. \quad (3)$$

The feature with the lowest mean correlation is selected:

$$Best\ f_i = \min(\text{mean}(C)). \quad (4)$$

This technique helps to minimize redundancy, enhancing model efficiency and performance [15, 18].

3.1.3. The minimum redundancy maximum relevance technique

The MRMR technique selects features by maximizing relevance to the target while minimizing redundancy among features [19–21]. Based on mutual information, it defines:

i. **Redundancy**:

$$Redundancy\ (S) = \frac{1}{|S|^2}\sum_{f_i,f_j S} I(f_i, f_j). \quad (5)$$

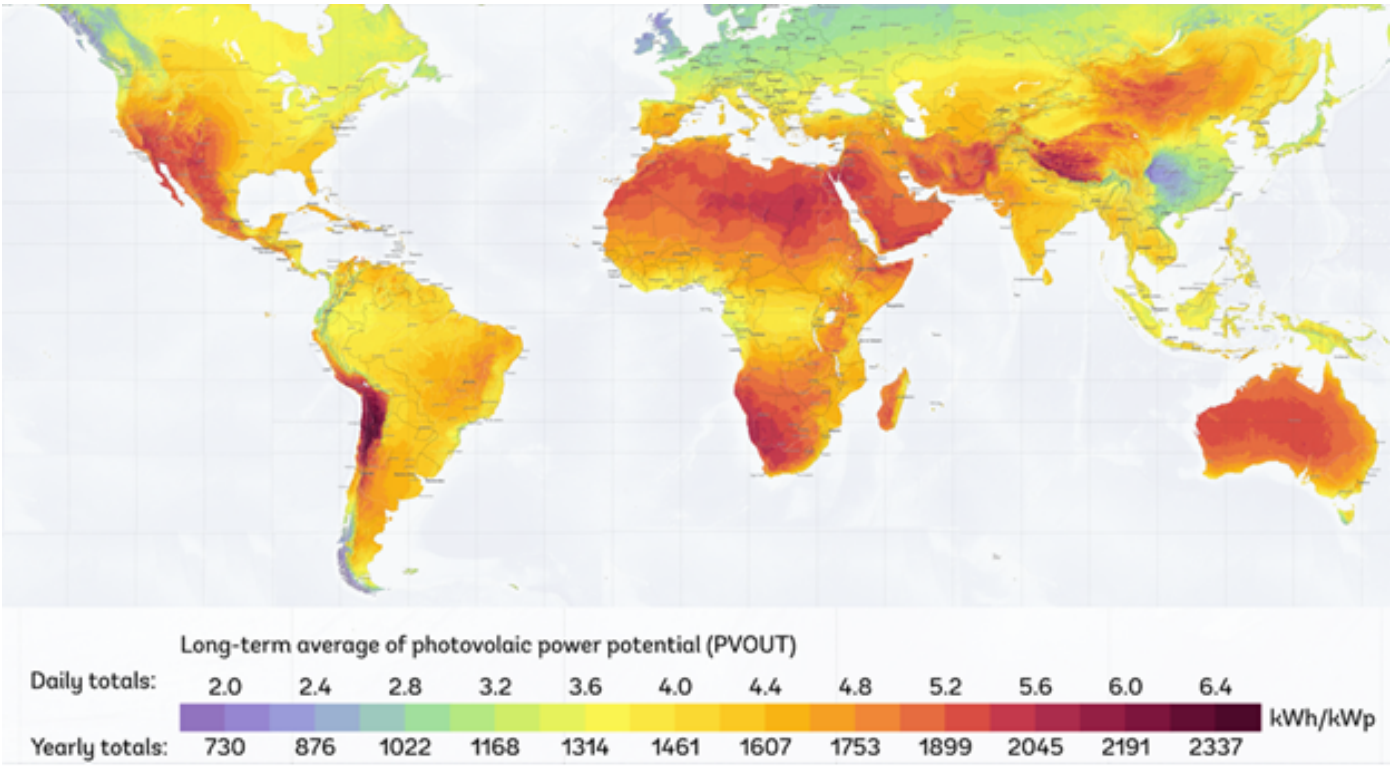

Figure 1. Practical photovoltaic power potential at level 2 (long-term average)[4].

Table 1. Summary of physical prediction methods.

Method	Description	Input Features	Authors	Advantages	Disadvantages
Simple Physical Model	Uses weather and system parameters for basic modeling	Weather data, solar radiation, satellite/cloud images, system parameters	Peder *et al.* [22]	Basic setup, conceptually straightforward	Low accuracy, needs detailed input data, lacks adaptability
Complex Physical Model	Incorporates advanced weather models with local data for improved prediction	NWP data, high-res weather maps, PV site-specific info	Lorenz *et al.* [23], Inman *et al.* [24]	Higher accuracy for local applications	Requires accurate weather forecasts and system characterization
NWP (Numerical Weather Prediction) Models	Use of mesoscale and global climate models for short- and wide-area forecasts	Wind speed, humidity, solar irradiance, etc.	Fernandez-Jimenez *et al.* [25], Mathiesen and Kleissl [26], Lima *et al.* [27]	Capable of large-area forecasting, weather-aware	High complexity, dependent on accurate weather models and computational resources

ii. **Relevance**:

$$Relevance\ (S,c) = \frac{1}{|S|} \sum_{f_i S} I(f_i, c) \tag{6}$$

where S is the set of features, c is the sample class, and f represents individual features in S. The optimal feature subset is determined by maximizing:

$$max\ \phi\ (Relevance, Redundancy) = Relevance - Redundancy \tag{7}$$

This balance between relevance and redundancy makes MRMR a powerful feature selection method for high-dimensional data.

3.2. *Variational Mode Decomposition (VMD)*

After identifying the key predictors for PV power forecasting, Variational Mode Decomposition is applied to decompose

Table 2. Summary of statistical prediction methods.

Method	Description	Input Features	Authors	Advantages	Disadvantages
Linear Regression (Unary/Multiple)	Establishes linear relationships between power output and influencing factors	Solar irradiance, temperature	Li *et al.* [28]	Easy to implement, interpretable models	Limited accuracy for nonlinear or complex dynamics
Support Vector Machine (SVM)	Uses kernel-based learning with generalization ability	Historical power, weather data	Li & Li (2008), Zhu & Tian [28]	Effective with limited data, avoids overfitting	Computational cost for large datasets
ARIMA / ARIMAX	Time series-based models for short-term forecasting	Historical PV output, solar irradiance	Pedro & Coimbra [29]	Handles time dependencies well	Ignores other weather-related variables
SARIMA	Seasonal ARIMA model for time series data	Historical PV output	Bouzerdoum *et al.* [30]	Improved accuracy with seasonality awareness	Still limited by weather variable exclusion
NARX / NARMAX	Nonlinear time-series models	Irradiance, temperature, time	Di Piazza *et al.* [31]	Captures nonlinearities effectively	Complex model formulation

Table 3. Summary of AI-based prediction methods.

Method	Description	Input features	Authors	Advantages	Disadvantages
BP Neural Network	Multi-layer network with backpropagation learning	Irradiance, temperature, time, historical power	Kaushika *et al.* [32]	Good performance with enough data	Requires large datasets, sensitive to overfitting
Extreme Learning Machine (ELM)	Fast learning single-layer feed-forward network	Historical power, weather data	Tang *et al.* [33]	High-speed learning, better generalization	Structure determination is difficult, less robust for small datasets
General Neural Networks	Deep learning or multilayer perceptrons (MLPs) with various optimization algorithms	Weather, system data, historical power	Various (Yang *et al.* [34]; Huang *et al.* [35])	Self-learning, adaptive to complex patterns	Risk of local minima, needs extensive tuning, not ideal for new/unknown scenarios without training data

the selected predictor into several Intrinsic Mode Functions (IMFs). This decomposition facilitates a detailed analysis of the impact of different numbers of IMFs on forecasting performance [36].

VMD aims to decompose a signal *f(t)* into a set of IMFs $\{u_k(t)\}$, each associated with a specific center frequency ω_k. The decomposition is formulated as the following optimization problem:

$$min_{\{uk\},\{\omega k\}} \left\{ \sum_k \left\| \partial_t (u_k(t) e^{-j\omega_k t}) \right\|_2^2 \right\}$$

$$\text{subject to} \quad \sum_k u_k(t) = f(t), \tag{8}$$

where $u_k(t)$ is the k-th mode, ω_k is the corresponding center frequency, ∂_t is the partial derivative with respect to time, j is the imaginary unit.

This process enables a refined exploration of the predictor's frequency components, enhancing the forecasting model's ability to capture underlying patterns.

3.3. Forecast models

To accurately forecast the photovoltaic power, five models are investigated including multilayer perceptron (MLP), Gated

Table 4. Review of State-of-the-Art Studies.

Authors	Focus	Method(s) used	Forecast horizon	Key findings / Notes
Wan *et al.* [12]	Review of forecasting methods	Statistical, AI, Physical, Hybrid approaches	Varies (very short to long-term)	Forecast category depends on data, horizon, and application. Hybrid models combine strengths of others.
Antonanzas *et al.* [13]	Comprehensive review of solar prediction research	Classification by time horizon, input data, and forecast types	Second to weeks	Compared point vs probabilistic forecasts; metrics for performance measurement reviewed.
Van der Meer *et al.* [14]	Probabilistic solar and load forecasting	Various probabilistic methods	Not specified	No one model fits all; variability between load and production can differ despite similar spatial/temporal resolutions.
Hong *et al.* [37]	GEFCom2014 competition	GB, k-NN, QRF, MQR, RF, SVM	24-hour forecast	Standardized datasets/metrics; top performers used machine learning (GB + k-NN).
Russo *et al.* [38]	Short-term forecasting (1 hour ahead)	Genetic algorithm + "The Brain Project"	1 hour	Algorithms with 2 inputs outperformed naïve ones.
Rana *et al.* [39]	Short-term PV production forecasting	ANN, SVM (Univariate & Multivariate)	Short-term	Univariate approach (production data only) had better accuracy (MAPE 4.15%–9.34%).
Li *et al.* [40]	PV park forecasting in Florida	ANN, SVR with hierarchical model	15 min, 1h, 24h	Aggregated inverter-level forecasts improved park-level predictions.
Golestaneh *et al.* [41]	Probabilistic solar forecasting	Extreme Learning Machine (ELM)	Minutes to 1 hour	ELM provides both point and probabilistic forecasts; tested across diverse climates.
Bessa *et al.* [42]	Probabilistic forecast over 6-hour horizon	Ensemble approach using multiple PV curves	6 hours	Combined data improved accuracy by 8%–12% vs univariate model.
Hosain *et al.* [43]	1-hour and 1-day solar production forecast	ELM vs ANN and SVR	1 hour, 1 day	ELM outperformed others in both accuracy and computation time.
Lonij *et al.* [44]	Forecast under cloudy skies using spatial correlation	Sensor-based spatial correlations	15-minute intervals	Outperformed naïve and satellite image-based models.
Vaz *et al.* [45]	Forecasting up to one month	NARX	>15 min to 1 month	Historical data from nearby PV farms improved accuracy; better than naïve model.
Lin and Pai [40]	Monthly production forecast in Taiwan	Seasonal Decomposition (SD) + LS-SVR with Genetic Algorithm	Monthly	SD improved accuracy significantly (MAPE 7.84%); LS-SVR+SD outperformed ARIMA, SARIMA, ANN, LSSVR without SD.

Recurrent Units (GRU), Long-Short Term Memory (LSTM), Bidirectional BiLSTM, and Convolutional Neural Network (CNN).

3.3.1. Multi-Layer Perceptron (MLP)

A Multi-Layer Perceptron (MLP) is a type of artificial neural network (ANN) composed of multiple layers of interconnected neurons. These layers include an input layer, one or more hidden layers, and an output layer. Each neuron in a layer is fully connected to the neurons in the adjacent layers, with each connection associated with a specific weight [2]. MLPs employ nonlinear activation functions in the hidden layers to capture complex patterns in the data. A general structure of the MLP model is illustrated in Figure 3.

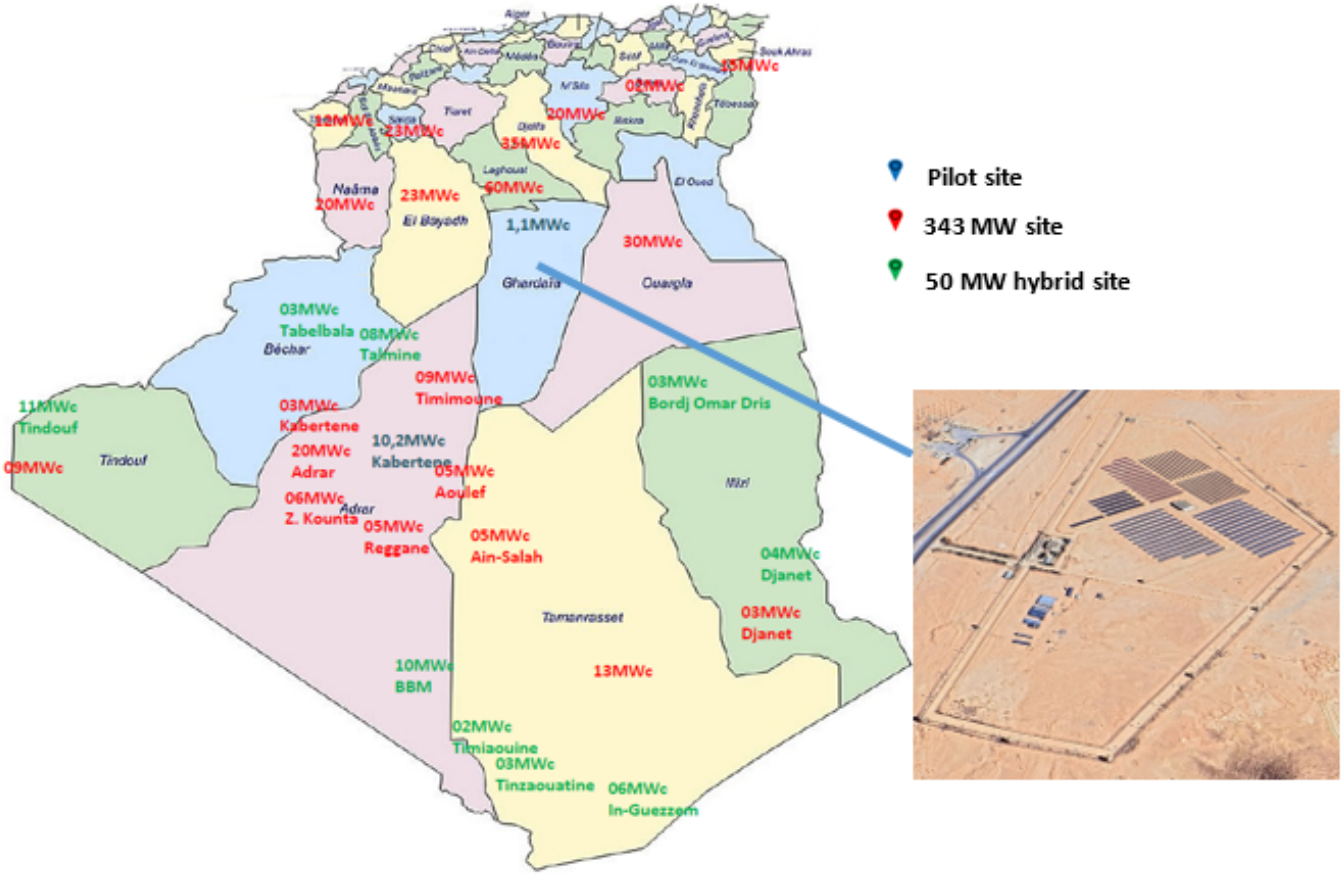

Figure 2. Studied site' location of the PV central.

3.3.2. *Gated Recurrent Unit (GRU)*

The Gated Recurrent Unit (GRU) is a type of recurrent neural network (RNN) architecture introduced to address the vanishing gradient problem observed in standard RNNs. GRUs are designed to capture dependencies in sequential data by using gating mechanisms that regulate the flow of information. Specifically, a GRU combines the hidden state and memory cell into a single unit and introduces two gates: the update gate and the reset gate [46]. These gates determine how much of the past information should be carried forward and how much should be forgotten. The relatively simple structure of GRUs allows for faster training and comparable performance to LSTM networks. The architecture of a typical GRU model is depicted in Figure 4.

3.3.3. *Long Short-Term Memory (LSTM)*

Long Short-Term Memory (LSTM) networks, introduced by Hochreiter and Schmidhuber in 1997 [47], are a specialized type of recurrent neural network (RNN) designed to address the limitations of traditional RNNs, particularly the vanishing gradient problem. LSTM networks are capable of learning long-term dependencies by incorporating memory cells and gating mechanisms.

Each LSTM unit consists of a cell, an input gate, a forget gate [48], and an output gate. These gates regulate the flow of information into and out of the cell, allowing the network to selectively retain relevant information over extended time sequences while discarding irrelevant or outdated data [49]. This selective memory mechanism makes LSTM architectures highly effective for sequential data analysis and time-series forecasting tasks. The general architecture of the LSTM model is shown in Figure 5.

3.3.4. *Bidirectional Long Short-Term Memory (BiLSTM)*

The Bidirectional Long Short-Term Memory network is an enhanced version of the standard LSTM architecture, designed to process sequential data in both forward and backward directions. This dual-directional structure enables the model to access information from both past and future time steps, making it particularly effective for capturing intricate temporal dependencies [50].

In a BiLSTM, two independent LSTM networks are trained in parallel: one processes the input sequence from start to end, while the other processes it in reverse. Their outputs are then combined—typically through concatenation—to produce a more contextually informed final prediction [51].

This architecture is widely applied in various domains such as energy forecasting, natural language processing, and time-

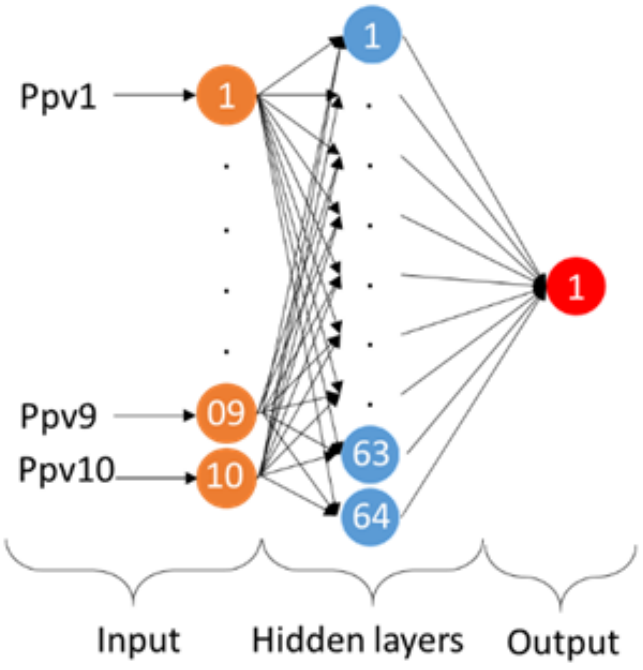

Figure 3. MLP architecture.

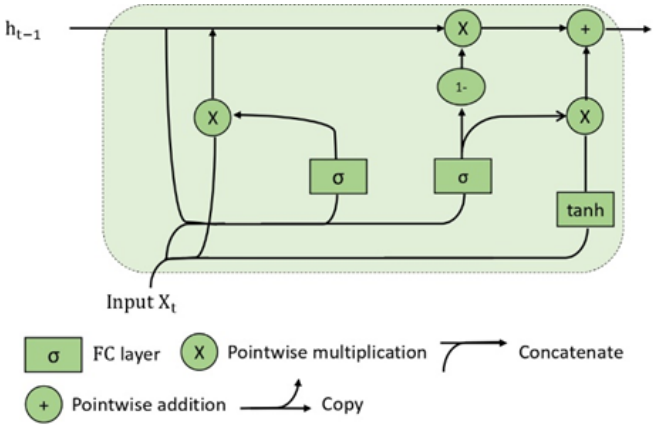

Figure 4. GRU architecture.

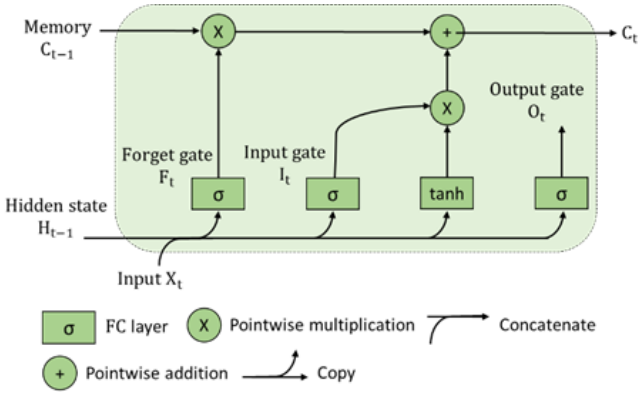

Figure 5. LSTM architecture.

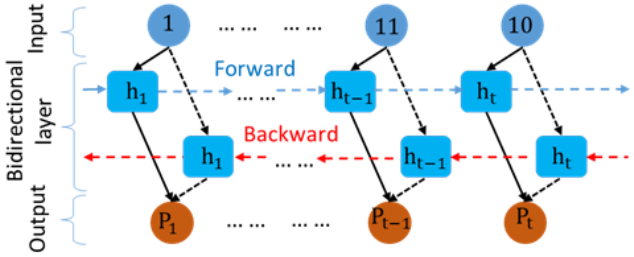

Figure 6. LSTM architecture.

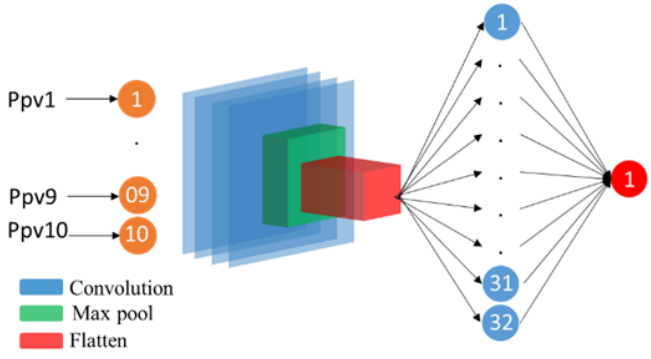

Figure 7. CNN architecture.

series analysis due to its ability to leverage bidirectional context [52–56]. An illustration of the BiLSTM model is presented in Figure 6.

3.3.5. *Convolutional Neural Network (CNN)*

Convolutional Neural Networks (CNNs) are a powerful class of deep learning models initially developed for image classification tasks [57, 58], but they have since been successfully adapted for time-series prediction in various domains, including energy forecasting [59], sizing of PV system [60], speech and face recognition [61], and prediction of data in PV applications [62].

The architecture of a CNN typically consists of a sequence of convolutional layers that apply learnable filters to extract spatial or temporal features, followed by pooling layers that reduce the dimensionality of feature maps [63]. These layers are often followed by fully connected layers for final output generation [64, 65]. A key advantage of CNNs is their ability to perform automatic feature extraction with minimal preprocessing, enabling efficient end-to-end learning [66–68].

In the context of PV power forecasting, CNNs can effectively capture localized temporal patterns in sequential data, improving the model's ability to generalize and predict power output. The CNN architecture used in this study is depicted in Figure 7.

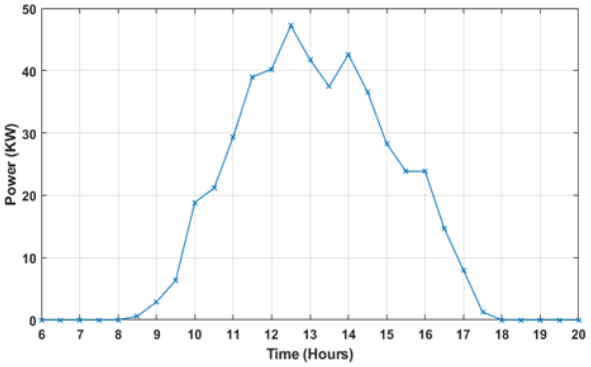

Figure 8. PV power variation in function of the time for a period of one day (01/01/2018).

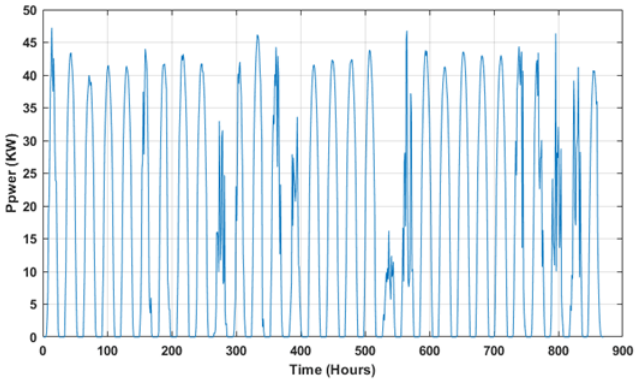

Figure 9. PV power variation in function of the time for a period of one Month (January 2018).

4. Experimental setup

In this section, we present insights into the dataset used for analysis, along with the data normalization process. Additionally, we describe the configuration of the forecasting models (MLP, GRU, LSTM, BiLSTM, and CNN) employed in this work. Finally, we discuss the evaluation metrics adopted to assess the robustness and predictive accuracy of the proposed models.

4.1. Data pre processing

As outlined in the previous section, the dataset comprises multiple input features, including temperature and global irradiation, and a single output representing PV power. In this study, each feature undergoes linear scaling to normalize its values within the range [0, 1], following the equation:

$$min_{\{uk\},\{\omega k\}} \left\{ \sum_k \left\| \partial_t (u_k(t) e^{-j\omega_k t}) \right\|_2^2 \right\} \quad (9)$$
$$\text{subject to} \quad \sum_k u_k(t) = f(t),$$

where X denotes the input feature vector, X_i^{nor} is the normalized value of featureX_i, $\max(X)$ and $\min(X)$ are the minimum and maximum values of X, respectively.

The output variable (PV power) is similarly normalized within the [0,1] range.

Following normalization, the dataset is split into three subsets: 70% for training, 15% for validation, and 15% for testing. The training set is used to optimize model parameters, the validation set helps prevent overfitting, and the test set evaluates the model's generalization capability.

Figures 8 and 99 illustrate samples of the PV power variations over time: Figure 8 shows the PV power variation over a single day (January 1, 2018) and Figure 9 shows the PV power variation over an entire month (January 2018).

These figures offer valuable insight into the temporal variability of photovoltaic (PV) power generation, a key factor in developing reliable forecasting models.

Figure 8 presents the PV power output for a single day—January 1, 2018. The curve shows a typical bell-shaped pattern, with power starting from zero at sunrise, increasing gradually to a peak around solar noon, and then decreasing back to zero at sunset. This pattern reflects clear sky conditions, as the smooth curve lacks sudden fluctuations, suggesting minimal impact from transient weather events such as cloud cover. This daily profile is essential for short-term forecasting models, especially those targeting hourly predictions.

Figure 9, on the other hand, illustrates the PV power variation over the entire month of January 2018. Unlike the single-day profile, the monthly curve displays significant variability from day to day. Some days exhibit high and smooth power generation, similar to the pattern seen in Figure 8, while others show reduced or irregular output, indicating the presence of cloudy or overcast conditions. This variability emphasizes the challenge in medium- to long-term forecasting and highlights the importance of incorporating meteorological data—such as irradiation and temperature—into the prediction models. It also underlines the need for robust models capable of generalizing across varying conditions.

4.2. PV forecast setup

The configuration settings for each forecasting model (MLP, GRU, LSTM, BiLSTM, and CNN) are summarized in **Table 5**. The MLP, GRU, LSTM, and BiLSTM models share a similar structure with three layers containing 64, 32, and 16 units, respectively, with the Rectified Linear Unit (ReLU) activation function.For the CNN model, three consecutive Conv1D layers are utilized with filter sizes of 64, 32, and 16, a kernel size of 2, and ReLU activation. All models were trained using the following parameters mentioned in Table 5.

4.3. Models Validation

Although the mathematical formulations of common error metrics can be found in previous studies [69, 70], this section highlights their physical interpretation and the improvements they provide.In this work, six statistical metrics are used to evaluate the forecasting performance of the models: RMSE, MAE,

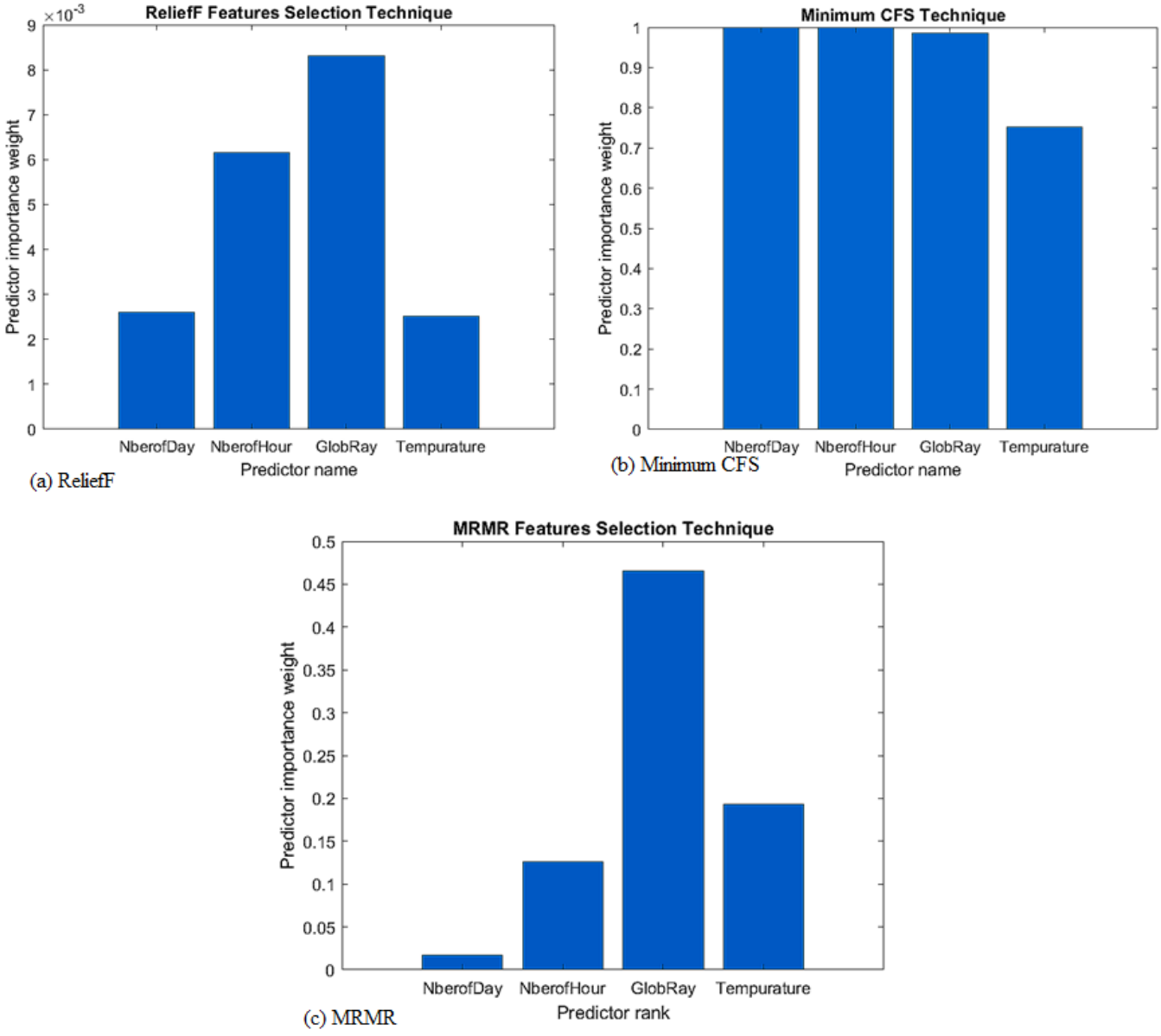

Figure 10. Predictors' importance Scores of the 4 predictors of the training input data of the used features selection techniques.

normalized RMSE (nRMSE), normalized MAE (nMAE), the Coefficient of Determination (R^2), and the Correlation Coefficient (R).

These metrics offer a comprehensive and scale-independent evaluation of model accuracy, allowing for effective comparison across different algorithms.

4.3.1. Root Mean Square Error (RMSE)

The Root Mean Square Error (RMSE) measures the standard deviation of prediction errors, giving greater weight to larger errors. It is defined as:

$$RMSE = \sqrt{\frac{1}{n}\sum_{i=1}^{n}(H_E - H_M)^2}, \tag{10}$$

where H_E is the estimated (predicted) value, H_M is the measured (actual) value, n is the total number of samples. Lower RMSE values indicate better forecasting performance.

4.3.2. Mean Absolute Error (MAE)

The Mean Absolute Error (MAE) quantifies the average magnitude of errors in a set of predictions, without considering their direction. It is given by:

$$MAE = \frac{1}{n}\sum_{i=1}^{n}|H_E - H_M|. \tag{11}$$

Unlike RMSE, MAE treats all errors equally, providing a direct measure of prediction accuracy.

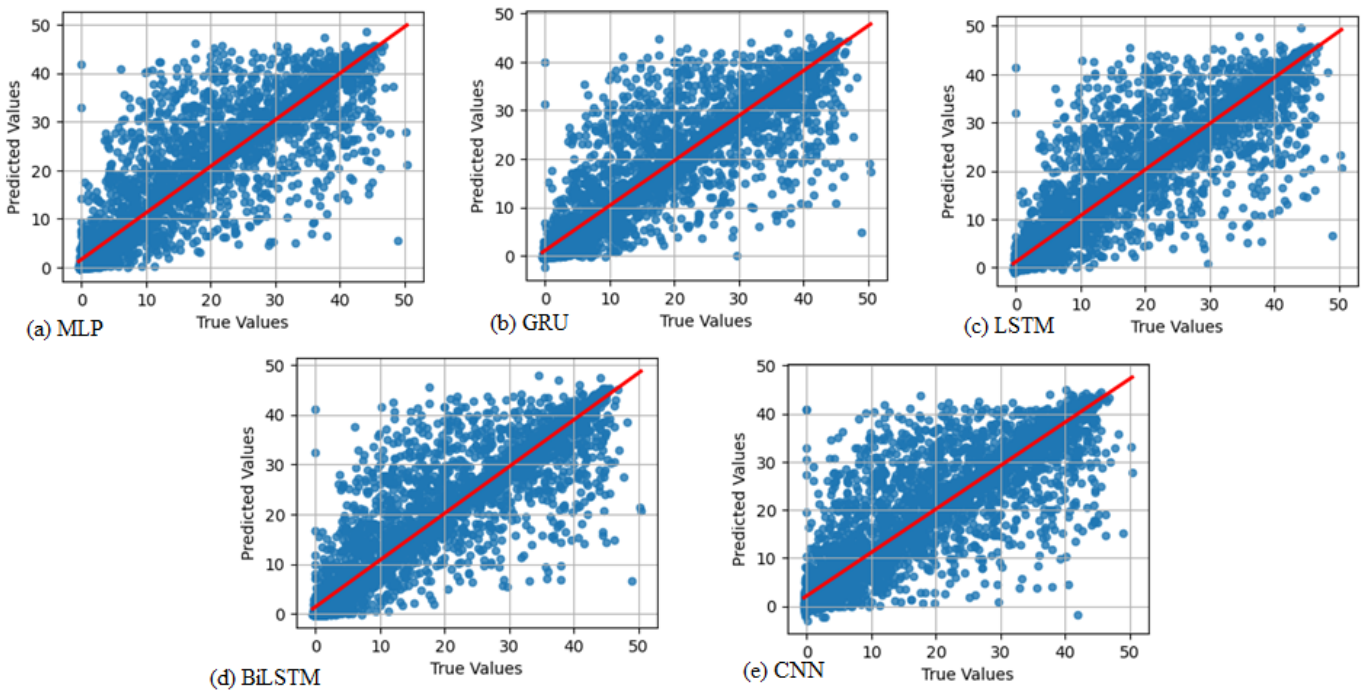

Figure 11. Correlation between measured and predicted PV power using 5 forecast models.

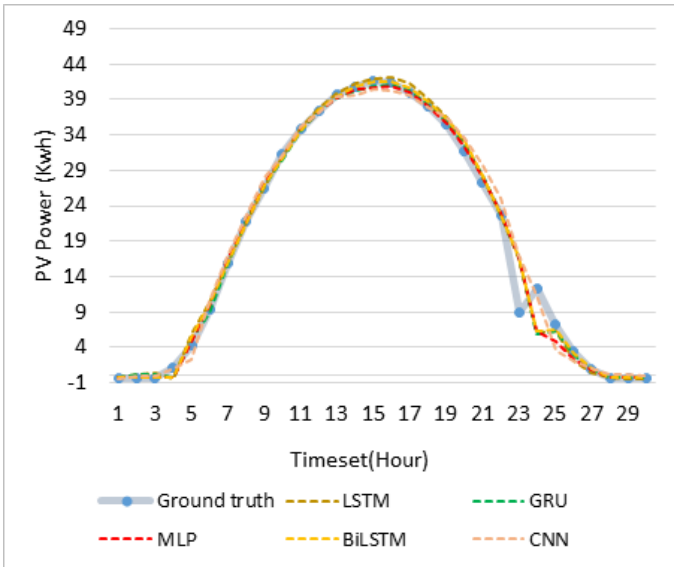

Figure 12. Forecast results on a typical sunny day.

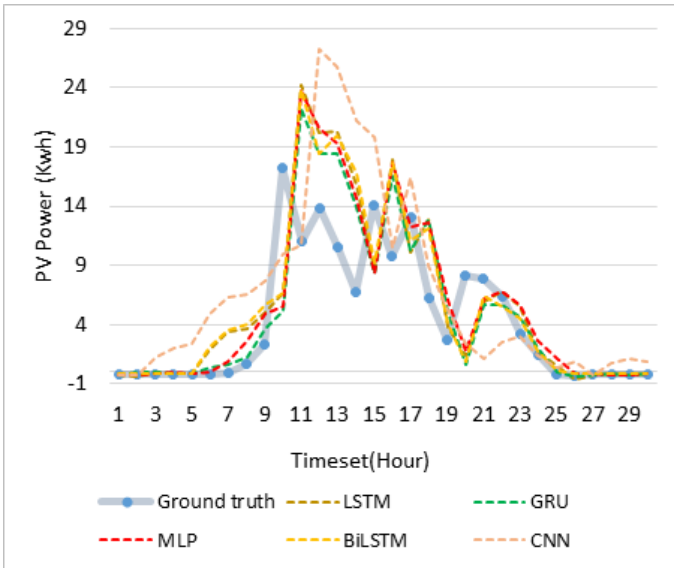

Figure 13. Forecast results on a typical cloudy day.

4.3.3. Normalized RMSE (nRMSE)

The normalized RMSE (nRMSE) expresses the RMSE as a percentage of the mean of the measured values, providing a scale-independent measure:

$$nRSME = \left(\frac{RMSE}{H_{Max} - H_{Min}}\right) \times 100. \quad (12)$$

The ranges of nRMSE define the model performance as [71, 72]: Excellent if: nRMSE $< 10\%$, Good if: $10\% <$ nRMSE $< 20\%$, Fair if: $20\% <$ nRMSE $< 30\%$, Poor if: nRMSE $> 30\%$.

4.3.4. Normalized MAE (nMAE)

Similarly, the normalized MAE (nMAE) relates the MAE to the mean of the measured values:

$$nMAE = \left(\frac{MAE}{\frac{1}{n}\sum_{i=1}^{n} H_M}\right) \times 100. \quad (13)$$

This metric also provides a percentage error independent of the data scale.

Table 5. Parameters of forecast models.

Model	Parameters	Values or properties
MLP	Number of hidden layers	3
	Size of hidden layers	64/32/16
	Activation function	ReLU
GRU	Number of layers	3
	LSTM cells in layer 1	64/32/16
	Activation function	ReLU
LSTM	Number of layers	3
	LSTM cells	64/32/16
	Activation function	ReLU
BiLSTM	Number of layers	3
	BiLSTM cells	64/32/16
	Activation function	ReLU
CNN	Number Conv1D layers	3
	Number of filters	64/32/16
	Kernel size	2
	Activation function	ReLU
Learning parameters		
Number of epochs	50	
Batch size	32	
Optimizer	Adam	
Learning rate	0.001	

4.3.5. Coefficient of Determination (R^2)

The Coefficient of Determination (R^2) assesses how well the predicted values approximate the actual data. It is defined by:

$$R^2 = 1 - \frac{\sum_{i=1}^{n} (H_M - H_E)^2}{\sum_{i=1}^{n} \left(H_M - \overline{H}_M\right)^2}, \tag{14}$$

where $\overline{H}_M$ is the mean of the measured values. An R^2 value closer to 1 indicates a stronger fit between the predicted and observed data.

4.3.6. Correlation Coefficient (R)

The Pearson Correlation Coefficient RRR quantifies the linear relationship between the predicted and measured values:

$$R = \frac{\sum_{i=1}^{n} \left(H_E - \overline{H}_E\right).\left(H_M - \overline{H}_M\right)}{\sqrt{\sum_{i=1}^{n} \left(H_E - \overline{H}_E\right). \sum_{i=1}^{n} \left(H_M - \overline{H}_M\right)}}, \tag{15}$$

where $\overline{H}_E$ and $\overline{H}_M$ are the mean predicted and measured values, respectively. An R value close to 1 signifies a strong positive correlation.

5. Results and discussion

The core focus of this study is to examine the critical impact of input predictor selection on the accuracy of photovoltaic (PV) power forecasting. As detailed in Section 4.1, the dataset comprises several potential predictors, including Global Solar Radiation, Number of Hours, Temperature, and Number of Days. However, utilizing all available features may lead to increased data dimensionality and introduce redundant or irrelevant information, which can degrade model performance and complicate the forecasting process. To address this, the study aims to systematically evaluate a range of feature selection techniques to identify the most relevant predictors, thereby enhancing the accuracy and efficiency of daily PV power prediction.

Figure 10 provides a comprehensive illustration of the ranking scores assigned to the four predictors within the training dataset, evaluated using a diverse set of feature selection techniques. These techniques—ReliefF, Minimum Correlation, and Minimum Redundancy Maximum Relevance (MRMR)—offer distinct analytical perspectives on the relative importance of each predictor in the context of photovoltaic (PV) power forecasting. By leveraging these complementary methods, the analysis highlights the varying degrees of influence that each input variable exerts on prediction accuracy.

The ReliefF feature selection technique identifies global solar radiation as the most significant predictor, with a score of 0.0082. Following closely is the hour number feature, scoring 0.0061. Conversely, both the day number and temperature features rank lower, each obtaining an equivalent score of 0.0025.

In contrast, the Minimum Correlations technique highlights "number of day" and "Number of Hour" as the most influential predictors, both scoring 1. This is followed by the Global solar radiation feature, which obtains a score of 0.98. The least compelling feature, according to this technique, is "Temperature", scoring 0.75.

The MRMR feature selection technique prioritizes "global solar radiation" as the most interesting feature, scoring 0.47, followed by "Temperature" at approximately 0.18. The predictor with the lowest importance score is "Number of the Day", scoring 0.02.

Table 6 serves as a comprehensive overview for understanding the comparative importance of the four predictors under investigation across various feature selection methodologies. The inclusion of the "Mean rank" column offers valuable insights into the overall ranking consensus achieved through the aggregation of results from multiple techniques.

Upon closer examination of the table, it becomes evident that "Global Solar Radiation" consistently garners significant attention across all feature selection approaches. With a mean rank of 2, this predictor attains a prominent position, standing out as a pivotal factor in predicting PV power production. Its recurrent prominence, securing the top rank in two techniques and a notable third place in one, underscores its robust influence on the predictive models.

Following the lead is the "Number of the Hour" feature, which maintains a commendable mean rank of 2. This observation underscores its substantive contribution to the predictive accuracy of the models, positioning it as a crucial determinant in forecasting PV power output.

Conversely, the "Number of the Day" predictor exhibits a comparatively weaker performance, as reflected by its mean

Table 6. Ranking of each of the four predictors according to Features selectors.

Predictor	Ranking according to			Mean Rank	Ranking according to Mean rank
	ReleifF	Min Correlation	MRMR		
N Day	3	2	4	3	3
N Hour	2	1	3	2	2
GSR	1	3	1	1,6666	1
T	4	4	2	3.3333	4

Table 7. Performance of daily PV Power forecasting without decomposition.

Model	RMSE	MAE	nRMSE	nMAE	R_square	R
MLP	5.0565	2.3520	9.9615	13.57	0.8908	0.9438
GRU	4.9558	2.3237	9.7632	13.41	0.8951	0.9461
LSTM	5.0128	2.2883	9.8755	13.20	0.8927	0.9448
BiLSMT	4.9740	2.3497	9.7991	13.56	0.8944	0.9457
CNN	5.7461	2.9761	11.3201	17.17	0.8590	0.9268

Table 8. The performance of daily PV Power forecasting in function of the number of IMFs using different forecasting models.

	Number of IMFs	RMSE	MAE	nRMSE	nMAE	R_square	R
ANN	1	5.0565	2.3520	9.9615	13.57	0.8908	0.9438
	2	4.3986	2.2317	8.6654	12.88	0.9174	0.9587
	3	3.9151	1.9225	7.7129	11.09	0.9346	0.9667
	4	3.6704	1.9288	7.2309	11.13	0.9425	0.9708
	5	3.2675	1.7258	6.4372	9.96	0.9544	0.9769
GRU	1	4.9558	2.3237	9.7632	13.41	0.8951	0.9461
	2	4.3026	2.1089	8.4763	12.17	0.9210	0.9597
	3	3.6191	1.7586	7.1299	10.15	0.9441	0.9716
	4	3.4056	1.6481	6.7092	9.51	0.9505	0.9749
	5	3.2460	1.6025	6.3948	9.25	0.9550	0.9772
LSTM	1	5.0128	2.2883	9.8755	13.20	0.8927	0.9448
	2	4.4186	2.1831	8.7049	12.60	0.9166	0.9574
	3	3.9612	2.1403	7.8038	12.35	0.9330	0.9659
	4	3.5886	1.8379	7.0697	10.60	0.9450	0.9721
	5	3.2482	1.6033	6.3990	9.25	0.9550	0.9772
BiLSTM	1	4.9740	2.3497	9.7991	13.56	0.8944	0.9457
	2	4.3316	2.0749	8.5334	11.97	0.9199	0.9591
	3	4.0508	2.0461	7.9802	11.81	0.9299	0.9643
	4	3.7166	1.8460	7.3220	10.65	0.9410	0.9701
	5	3.2750	1.6669	6.4519	9.62	0.9542	0.9768
CNN	1	5.7461	2.9761	11.3201	17.17	0.8590	0.9268
	2	4.7728	2.5586	9.4027	14.76	0.9027	0.9501
	3	4.8968	2.8528	9.6470	16.46	0.8976	0.9474
	4	4.2006	2.4455	8.2754	14.11	0.9247	0.9616
	5	4.0967	2.2994	8.0708	13.27	0.9283	0.9635

rank of 3. While still contributing to the predictive process, its lower ranking suggests that it may not wield as much influence as the other predictors in the dataset.

Table 7 presents the performance of different models for daily PV power forecasting using the "Global solar radiation" feature. Among the models, GRU achieves the best overall performance, showing the lowest RMSE (4.9558) and MAE (2.3237), along with the highest R^2 and R. LSTM and BiLSTM also perform well, with errors close to GRU but slightly higher. MLP, although slightly behind GRU, still shows strong performance, particularly with a solid R^2 value of 0.8908. CNN, in contrast, shows the weakest performance, having the highest RMSE (5.7461) and MAE (2.9761), along with the lowest R^2 (0.8590), suggesting it is less reliable for forecasting daily PV

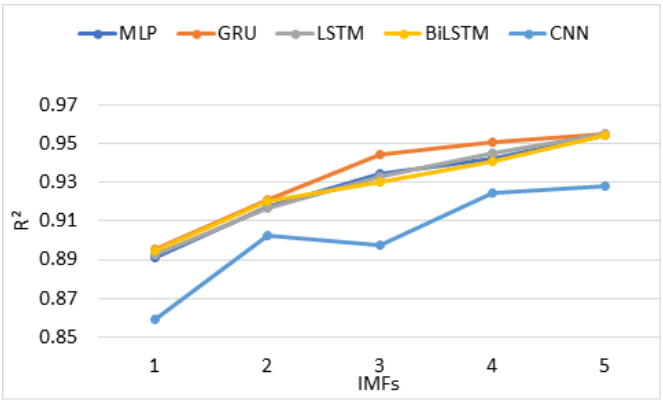

Figure 14. R^2 in function of the number of IMFs for the forecast models.

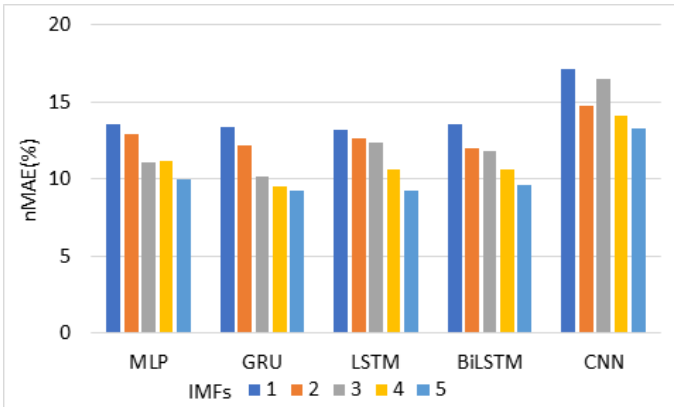

Figure 15. The nMAE in function of the number of IMFs for the forecast models.

power compared to the recurrent neural network-based models. Overall, models based on recurrent architectures including GRU, LSTM and BiLSTM outperform the MLP and CNN models in this task.

Figure 11 exemplifies the regression between the measured and predicted daily PV Power using the forecast models. This illustration showcases the optimal results attained across all experiments, achieved through the forecast models using the selected predictor. Notably, the graph depicts minimal dispersion between the measured and predicted data points, underscoring the exceptional performance of our features selection approach.

Furthermore, Figure 12 shows the performance of different forecast models against the ground truth on a typical sunny day. Overall, MLP and GRU exhibit moderate performance with some deviations from the ground truth, particularly at lower values. LSTM and BiLSTM tend to perform well at higher values but show inaccuracies in the middle range. CNN has more significant fluctuations, especially for lower values, although it remains more stable at higher values. GRU and MLP are generally more consistent compared to LSTM and BiLSTM, which are more sensitive to value fluctuations.

Figure 13 presents the forecast of PV power on a typical rainy day, the models. The measured PV power fluctuates between negative and positive values, reflecting the varying solar power during cloudy conditions. The MLP and GRU models tend to underestimate the values in the beginning, especially in lower power readings, but show better alignment with the ground truth as the forecast progresses toward higher values. LSTM and BiLSTM perform well during periods of higher power but experience underestimation or large deviations in the lower and medium ranges, particularly for very low power values. CNN, while exhibiting high volatility, especially in the low power range, follows the trends better in the higher power regions. However, it struggles with sudden transitions from low to high values. Overall, the models' predictions vary widely in the early part of the day, where solar power is low, and are closer to the ground truth as the day progresses and the power output increases. CNN appears to perform the best in the higher power regions but faces challenges at the start, while MLP and GRU show more consistent performance throughout the forecast period.

Table 8 provides a quantitative assessment of the performance of five forecasting models including ANN, GRU, LSTM, BiLSTM, and CNN for PV power forecast, evaluated using various metrics: including RMSE, MAE, nRMSE, nMAE, R^2, and correlation (R), across different numbers of IMFs (1 to 5).

As the number of IMFs increases, all models demonstrate improvements in forecasting accuracy, reflected by a consistent decrease in RMSE and MAE, and an increase in R^2 and correlation values. For instance, in the ANN model, RMSE decreases from 5.0565 at 1 IMF to 3.2675 at 5 IMFs, while MAE drops from 2.3520 to 1.7258. Similarly, in GRU, RMSE reduces from 4.9558 to 3.2460, and MAE drops from 2.3237 to 1.6025. This trend is also observed in LSTM, BiLSTM, and CNN models.

Notably, GRU and LSTM consistently outperform the other models, achieving the lowest RMSE and MAE values, along with the highest R^2 values, particularly when 3 or more IMFs are used. For example, GRU shows an R^2 increase from 0.8951 at 1 IMF to 0.9550 at 5 IMFs, and LSTM similarly improves from 0.8927 to 0.9550. These models demonstrate stronger correlation between predicted and actual values, with GRU reaching a correlation of 0.9772 and LSTM matching that at 5 IMFs. In contrast, CNN shows the least accuracy across all metrics, with the highest RMSE and MAE values, indicating it is less effective in forecasting PV power compared to the other models.

Overall, increasing the number of IMFs enhances forecasting accuracy, improving both the fit of the model and the correlation between predicted and actual data. GRU and LSTM are the most effective models for PV power forecasting, achieving the lowest errors and the highest correlation and R^2 values as the number of IMFs increases.

Moreover, Figure 14 shows that increasing the number of IMFs generally improves the R^2 values for all models, indicating better data fitting. ANN performs the best, steadily increasing with more IMFs. GRU follows a similar pattern but with slightly lower values. LSTM and BiLSTM show similar improvements, plateauing after 4 IMFs. CNN starts lower but improves sharply, matching the other models by 5 IMFs. Overall, more IMFs enhance performance, with ANN achieving the

highest R-squared values.

Figure 15 reveals that as the number of IMFs increases, the nMAE error steadily decreases for all models. ANN, GRU, LSTM, and BiLSTM show a smooth and consistent decline, reflecting enhanced performance with more IMFs. GRU and BiLSTM, in particular, exhibit quicker improvements beyond the third IMF. CNN begins with the highest error and shows less stable behavior, though its error drops notably after the fourth IMF. Overall, ANN and GRU achieve the most stable and efficient error reduction as the number of IMFs grows.

6. Conclusion

This study proposes a robust, data-driven framework for enhancing daily photovoltaic (PV) power forecasting by integrating advanced feature selection techniques, signal decomposition, and deep learning models. The results underscore the pivotal role of feature selection in improving forecasting accuracy. Through the application and comparison of three feature selection methods—ReliefF, Minimum Correlation Feature Selection (CFS), and Minimum Redundancy Maximum Relevance (MRMR)—Global Solar Radiation (GSR) was consistently identified as the most influential predictor. Incorporating the selected features into the forecasting pipeline, along with Variational Mode Decomposition (VMD) as a preprocessing step, significantly improved model performance. Among the tested deep learning architectures, the Gated Recurrent Unit (GRU) network delivered the highest predictive accuracy, achieving an RMSE of 3.246 and an R^2 of 0.9550. Graphical evaluations further validated the model's reliability, demonstrating close alignment between predicted and actual values. Overall, the findings demonstrate that the integration of optimal feature selection and signal decomposition techniques with deep learning offers a highly effective strategy for improving the precision and robustness of PV power forecasting—particularly valuable for energy planning and management in solar-rich regions.

Data availability

The datasets used and/or analyzed during the current study are available from co-author Dr. Abdelaziz Rabehi (rab_ehi@hotmail.fr) on reasonable request.

Acknowledgements

The researchers wish to extend their sincere gratitude to the Deanship of Scientific Research at the Islamic University of Madinah (KSA) for the support provided to the Post-Publishing Program.

References

[1] M. W. Bouabdelli, F. Rogti, M. Maache & A. Rabehi, "Performance enhancement of CIGS thin-film solar cell, Optik (Stuttg)", **216** (2020) 164948. https://doi.org/10.1016/j.ijleo.2020.164948.

[2] M. Guermoui & A. Rabehi, "Soft computing for solar radiation potential assessment in Algeria", International Journal of Ambient Energy **41** (2020) 1524. https://doi.org/10.1080/01430750.2018.1517686.

[3] F. Bendelala, A. Bellakhdar, O. Baitiche, A. Cheknane, M.H.S. Helal, H.S. Hilal & A. Rabehi, "FDTD Modelling of Nanostructured Hemispherical Plasmonic Light Trapping for Enhanced Ultra-thin GaSb TPV Cell", Semiconductors **59** (2025) 404. https://doi.org/10.1134/S1063782624603029.

[4] M. Suri, J. Betak, K. Rosina, D. Chrkavy, N. Suriova, T. Cebecauer, M. Caltik & B. Erdelyi, "Global Photovoltaic Power Potential by Country (English)", 2020. [Online]. https://documents1.worldbank.org/curated/en/466331592817725242/pdf/Global-Photovoltaic-Power-Potential-by-Country.pdf.

[5] M. Guermoui, F. Melgani & C. Danilo, "Multi-step ahead forecasting of daily global and direct solar radiation: A review and case study of Ghardaia regi", J Clean Prod **201** (2018) 716. https://doi.org/10.1016/j.jclepro.2018.08.006.

[6] A. Mehallou, B. M'hamdi, A. Amari, M. Teguar, A. Rabehi, M. Guermoui, A. H. Alharbi, E.-S. M. El-kenawy & D. S. Khafaga, "Optimal multiobjective design of an autonomous hybrid renewable energy system in the Adrar Region, Algeria", Sci Rep **15** (2025) 4173. https://doi.org/10.1038/s41598-025-88438-x.

[7] A. Belaid, A. Filali, S. Hassani, T. Arrif, M. Guermoui, A. Gama, M. Bouakba, "Heliostat field optimization and comparisons between biomimetic spiral and radial-staggered layouts for different heliostat shapes", Solar Energy **238** (2022) 162. https://doi.org/10.1016/j.solener.2022.04.035.

[8] H. Bentegri, M. Rabehi, S. Kherfane, T. A. Nahool, A. Rabehi, M. Guermoui, A. A. Alhussan, D. S. Khafaga, M. M. Eid, E.-S.M. El-Kenawy, "Assessment of compressive strength of eco-concrete reinforced using machine learning tools", Sci Rep **15** (2025) 5017. https://doi.org/10.1038/s41598-025-89530-y.

[9] M. Mahmoud Al Rahhal, M. L. Mekhalfi, M. Guermoui, E. Othman, B. Lei & A. Mahmood, "A dense phase descriptor for human ear recognition", IEEE Access **6** (2018) 11883. https://doi.org/10.1109/ACCESS.2018.2810339.

[10] M. Guermoui, M. L. Mekhalfi & K. Ferroudji, "Heart sounds analysis using wavelets responses and support vector machines, in: 2013 8th International Workshop on Systems", Signal Processing and their Applications (WoSSPA), IEEE, Algiers, Algeria, 2013, pp. 233–238. https://doi.org/10.1109/WoSSPA.2013.6602368.

[11] M. Guermoui, T. Arrif, A. Belaid, S. Hassaniv & N. Bailek, "Enhancing direct Normal solar Irradiation forecasting for heliostat field applications through a novel hybrid model", Energy Convers Manag **304** (2024) 118189. https://doi.org/10.1016/j.enconman.2024.118189.

[12] C. Wan, J. Zhao, Y. Song, Z. Xu, J. Lin & Z. Hu, "Photovoltaic and solar power forecasting for smart grid energy management", CSEE Journal of Power and Energy Systems **1** (2015) 38. https://doi.org/10.17775/CSEEJPES.2015.00046.

[13] J. Antonanzas, N. Osorio, R. Escobar, R. Urraca, F.J. Martinez-de-Pison, F. Antonanzas-Torres, Review of photovoltaic power forecasting, Solar Energy **136** (2016) 78. https://doi.org/10.1016/j.solener.2016.06.069.

[14] D. W. van der Meer, J. Widén & J. Munkhammar, "Review on probabilistic forecasting of photovoltaic power production and electricity consumption", Renewable and Sustainable Energy Reviews **81** (2018) 1484. https://doi.org/10.1016/j.rser.2017.05.212.

[15] X. Huang, H. Wang & X. Li, "A multi-scale semantic feature fusion method for remote sensing crop classification", Comput Electron Agric **224** (2024) 109185. https://doi.org/10.1016/j.compag.2024.109185.

[16] K. Kira & L. A. Rendell, "A Practical Approach to Feature Selection", Machine Learning Proceedings **1992** (1992) 249. https://doi.org/10.1016/B978-1-55860-247-2.50037-1.

[17] A. Chennana, A. C. Megherbi, N. Bessous, S. Sbaa, A. Teta, E. O. Belabbaci, A. Rabehi, M. Guermoui & T. F. Agajie, "Vibration signal analysis for rolling bearings faults diagnosis based on deep-shallow features fusion", Sci Rep **15** (2025) 9270. https://doi.org/10.1038/s41598-025-93133-y.

[18] R. Khelifi, T. Chekifi, A. Belaid, M. Guermoui, A. Rabehi, F. Khaled, M. Adouane, A. Al-Qattan & T. F. Agajie, "Comparative performance analysis of hemispherical solar stills using date and olive kernels as heat storage material", Sci Rep **15** (2025) 7128. https://doi.org/10.1038/

s41598-025-87448-z.

[19] I. E. Tibermacine, A. Douara, M. Guermoui, A. Rabehi, O. Baitiche, A. Boualleg, E. Mehallel & S. Boukredine, "Enhanced Performance of Microstrip Antenna Arrays through Concave Modifications and Cut-Corner Techniques", ITEGAM- Journal of Engineering and Technology for Industrial Applications (ITEGAM-JETIA **11** (2025) 1414. https://doi.org/10.5935/jetia.v11i51.1414.

[20] H. Peng, F. Long & C. Ding, "Feature selection based on mutual information criteria of max-dependency, max-relevance, and min-redundancy", IEEE Trans Pattern Anal Mach Intell **27** (2005) 1226. https://doi.org/10.1109/TPAMI.2005.159.

[21] B. Ladjal, I. E. Tibermacine, M. Bechouat, M. Sedraoui, C. Napoli, A. Rabehi & D. Lalmi, "Hybrid models for direct normal irradiance forecasting: a case study of Ghardaia zone (Algeria)", Natural Hazards **120** (2024) 14703. https://doi.org/10.1007/s11069-024-06837-1.

[22] P. Bacher, H. Madsen & H. A. Nielsen, "Online short-term solar power forecasting", Solar Energy **83** (2009) 1772. https://doi.org/10.1016/j.solener.2009.05.016.

[23] E. Lorenz, T. Scheidsteger, J. Hurka, D. Heinemann & C. Kurz, "Regional PV power prediction for improved grid integration", Progress in Photovoltaics: Research and Applications **19** (2011) 757. https://doi.org/10.1002/pip.1033.

[24] R. H. Inman, H. T. C. Pedro & C. F. M. Coimbra, "Solar forecasting methods for renewable energy integration", Prog Energy Combust Sci **39** (2013) 535. https://doi.org/10.1016/j.pecs.2013.06.002.

[25] L. A. Fernandez-Jimenez, A. Muñoz-Jimenez, A. Falces, M. Mendoza-Villena, E. Garcia-Garrido, P. M. Lara-Santillan, E. Zorzano-Alba & P. J. Zorzano-Santamaria, "Short-term power forecasting system for photovoltaic plants", Renew Energy **44** (2012) 311. https://doi.org/10.1016/j.renene.2012.01.108.

[26] P. Mathiesen, J. Kleissl, Evaluation of numerical weather prediction for intra-day solar forecasting in the continental United States, Solar Energy **85** (2011) 967. https://doi.org/10.1016/j.solener.2011.02.013.

[27] F. J. L. Lima, F. R. Martins, E. B. Pereira, E. Lorenz & D. Heinemann, "Forecast for surface solar irradiance at the Brazilian Northeastern region using NWP model and artificial neural networks", Renew Energy **87** (2016) 807. https://doi.org/10.1016/j.renene.2015.11.005.

[28] H. Ye, B. Yang, Y. Han & N. Chen, "State-Of-The-Art Solar Energy Forecasting Approaches: Critical Potentials and Challenges", Front Energy Res **10** (2022) 875790. https://doi.org/10.3389/fenrg.2022.875790.

[29] H.T.C. Pedro & C.F.M. Coimbra, "Assessment of forecasting techniques for solar power production with no exogenous inputs", Solar Energy **86** (2012) 2017. https://doi.org/10.1016/j.solener.2012.04.004.

[30] M. Bouzerdoum, A. Mellit & A. Massi Pavan, "A hybrid model (SARIMA–SVM) for short-term power forecasting of a small-scale grid-connected photovoltaic plant", Solar Energy **98** (2013) 226. https://doi.org/10.1016/j.solener.2013.10.002.

[31] A. Di Piazza, M. C. Di Piazza & G. Vitale, "Solar and wind forecasting by NARX neural networks", Renewable Energy and Environmental Sustainability **1** (2016) 39. https://doi.org/10.1051/rees/2016047.

[32] N. D. Kaushika, R. K. Tomar & S. C. Kaushik, "Artificial neural network model based on interrelationship of direct, diffuse and global solar radiations", Solar Energy **103** (2014) 327. https://doi.org/10.1016/j.solener.2014.02.015.

[33] P. Tang, D. Chen & Y. Hou, "Entropy method combined with extreme learning machine method for the short-term photovoltaic power generation forecasting", Chaos Solitons Fractals **89** (2016) 243. https://doi.org/10.1016/j.chaos.2015.11.008.

[34] B. Yang, T. Zhu, P. Cao, Z. Guo, C. Zeng, D. Li, Y. Chen, H. Ye, R. Shao, H. Shu & Tao Yu, "Classification and summarization of solar irradiance and power forecasting methods: A thorough review", CSEE Journal of Power and Energy Systems **9** (2021) 978. https://doi.org/10.17775/CSEEJPES.2020.04930.

[35] S. Huang, Q. Wu, W. Liao, G. Wu, X. Li & J. Wei, "Adaptive Droop-Based Hierarchical Optimal Voltage Control Scheme for VSC-HVdc Connected Offshore Wind Farm", IEEE Trans Industr Inform **17** (2021) 8165. https://doi.org/10.1109/TII.2021.3065375.

[36] M. Marzouglal, A. Souahlia, L. Bessissa, D. Mahi, A. Rabehi, Y.Z. Alharthi, A.K. Bojer, A. Flah, M.M. Alharthi, S. S. M. Ghoneim, "Prediction of power conversion efficiency parameter of inverted organic solar cells using artificial intelligence techniques", Sci Rep **14** (2024) 25931. https://doi.org/10.1038/s41598-024-77112-3.

[37] T. Hong, P. Pinson, S. Fan, H. Zareipour, A. Troccoli & R. J. Hyndman, "Probabilistic energy forecasting: Global Energy Forecasting Competition 2014 and beyond", Int J Forecast **32** (2016) 896. https://doi.org/10.1016/j.ijforecast.2016.02.001.

[38] M. Russo, G. Leotta, P. M. Pugliatti & G. Gigliucci, "Genetic programming for photovoltaic plant output forecasting", Solar Energy **105** (2014) 264. https://doi.org/10.1016/j.solener.2014.02.021.

[39] M. Rana, I. Koprinska & V. G. Agelidis, "Univariate and multivariate methods for very short-term solar photovoltaic power forecasting", Energy Convers Manag **121** (2016) 380. https://doi.org/10.1016/j.enconman.2016.05.025.

[40] K. P. Lin & P. F. Pai, "Solar power output forecasting using evolutionary seasonal decomposition least-square support vector regression", J Clean Prod **134** (2016) 456. https://doi.org/10.1016/j.jclepro.2015.08.099.

[41] F. Golestaneh, P. Pinson & H. B. Gooi, "Very short-term nonparametric probabilistic forecasting of renewable energy generation— with application to solar Energy", IEEE Transactions on Power Systems **31** (2016) 3850. https://doi.org/10.1109/TPWRS.2015.2502423.

[42] R. J. Bessa, A. Trindade, C. S. P. Silva & V. Miranda, "Probabilistic solar power forecasting in smart grids using distributed information", International Journal of Electrical Power & Energy Systems **72** (2015) 16. https://doi.org/10.1016/j.ijepes.2015.02.006.

[43] M. Hossain, S. Mekhilef, M. Danesh, L. Olatomiwa & S. Shamshirband," Application of extreme learning machine for short term output power forecasting of three grid-connected PV systems", J Clean Prod **167** (2017) 395. https://doi.org/10.1016/j.jclepro.2017.08.081.

[44] V. P. A. Lonij, A. E. Brooks, A. D. Cronin, M. Leuthold & K. Koch, "Intra-hour forecasts of solar power production using measurements from a network of irradiance sensors", Solar Energy **97** (2013) 58. https://doi.org/10.1016/j.solener.2013.08.002.

[45] A. G. R. Vaz, B. Elsinga, W.G.J.H.M. van Sark, "M.C. Brito, An artificial neural network to assess the impact of neighbouring photovoltaic systems in power forecasting in Utrecht", the Netherlands, Renew Energy **85** (2016) 631. https://doi.org/10.1016/j.renene.2015.06.061.

[46] R. Dey & F. M. Salem, "Gate-variants of Gated Recurrent Unit (GRU) neural networks", in *IEEE 60th International Midwest Symposium on Circuits and Systems (MWSCAS)*, Boston, MA, USA, 2017, pp. 1597–1600. https://doi.org/10.1109/MWSCAS.2017.8053243.

[47] S. Hochreiter & J. Schmidhuber, "Long Short-Term Memory", Neural Comput **9** (1997) 1735. https://doi.org/10.1162/neco.1997.9.8.1735.

[48] F. A. Gers & J. Schmidhuber, "Recurrent nets that time and count", Neural Computing **3** (2000) 189. https://doi.org/10.1109/IJCNN.2000.861302.

[49] H. Alizadegan, B. Rashidi Malki, A. Radmehr, H. Karimi, M. A. Ilani, "Comparative study of long short-term memory (LSTM), bidirectional LSTM, and traditional machine learning approaches for energy consumption prediction", Energy Exploration & Exploitation **43** (2025) 281. https://doi.org/10.1177/01445987241269496.

[50] K. Zhang, X. Huo & K. Shao, "Temperature time series prediction model based on time series decomposition and Bi-LSTM Network", Mathematics **11** (2023) 2060. https://doi.org/10.3390/math11092060.

[51] B. Jang, M. Kim, G. Harerimana, S. Kang & J. W. Kim, "Bi-LSTM model to increase accuracy in text classification: combining word2vec cnn and attention mechanism", Applied Sciences **10** (2020) 5841. https://doi.org/10.3390/app10175841.

[52] M. Guermoui, A. Rabehi, S. Benkaciali, D. Djafer, "Daily global solar radiation modelling using multi-layer perceptron neural networks in semi-arid region", Leonardo Electronic Journal of Practices and Technologies **28** (2016) 35. http://lejpt.academicdirect.org/A28/035_046.pdf.

[53] A. Rabehi, M. Guermoui, R. Khelifi & M. L. Mekhalfi, "Decomposing global solar radiation into its diffuse and direct normal radiation", International Journal of Ambient Energy **41** (2020) 738. https://doi.org/10.1080/01430750.2018.1492445.

[54] A. Rabehi, M. Guermoui & D. Lalmi, "Hybrid models for global solar radiation prediction: a case study", International Journal of Ambient Energy **41** (2020) 31. https://doi.org/10.1080/01430750.2018.1443498.

[55] N. El-Amarty, M. Marzouq, H. El Fadili, S. Dosse Bennani, A. Ruano, A. Rabehi, "A new evolutionary forest model via incremental tree selection for short-term global solar irradiance forecasting under six various climatic zones", Energy Convers Manag **310** (2024) 118471. https://doi.org/10.1016/j.enconman.2024.118471.

[56] A. Bouchakour, L. Zarour, N. Bessous, M. Bechouat, A. Borni, L. Zaghba, A. Rabehi, A. Alwabli, M. El-Abd, S. S. M. Ghoneim, "MPPT algorithm based on metaheuristic techniques (PSO & GA) dedicated to improve wind energy water pumping system performance", Sci Rep **14** (2024) 17891. https://doi.org/10.1038/s41598-024-68584-4.

[57] D. X. Zhou, "Theory of deep convolutional neural networks: Downsampling", Neural Networks **124** (2020) 319. https://doi.org/10.1016/j.neunet.2020.01.018.

[58] A. Krizhevsky, I. Sutskever & G. E. Hinton, "ImageNet classification with deep convolutional neural networks", Commun ACM **60** (2017) 84. https://doi.org/10.1145/3065386.

[59] W. Lu, J. Li, J. Wang & L. Qin, "A CNN-BiLSTM-AM method for stock price prediction", Neural Comput Appl **33** (2021) 4741. https://doi.org/10.1007/s00521-020-05532-z.

[60] T. Arrif, A. Benchabane, M. Guermoui, A. Gama & H. Merarda, "Optical performance study of different shapes of solar cavity receivers used in central receiver system plant", International Journal of Ambient Energy **42** (2021) 81. https://doi.org/10.1080/01430750.2018.1525584.

[61] D. Palaz, M. Magimai-Doss & R. Collobert, "End-to-end acoustic modeling using convolutional neural networks for HMM-based automatic speech recognition", Speech Commun **108** (2019) 15. https://doi.org/10.1016/j.specom.2019.01.004.

[62] B. Ladjal, M. Nadour, M. Bechouat, N. Hadroug, M. Sedraoui, A. Rabehi, M. Guermoui & T. F. Agajie, "Hybrid deep learning CNN-LSTM model for forecasting direct normal irradiance: a study on solar potential in Ghardaia, Algeria", Sci Rep **15** (2025) 15404. https://doi.org/10.1038/s41598-025-94239-z.

[63] A. Teta, B. Korich, D. Bakria, N. Hadroug, A. Rabehi, M. Alsharef, M. Bajaj, I. Zaitsev & S. S. M. Ghoneim, "Fault detection and diagnosis of grid-connected photovoltaic systems using energy valley optimizer based lightweight CNN and wavelet transform", Sci Rep **14** (2024) 18907. https://doi.org/10.1038/s41598-024-69890-7.

[64] A. Rabehi, B. Nail, H. Helal, A. Douara, A. Ziane, M. Amrani, B. Akkal & Z. Benamara, "Optimal estimation of Schottky diode parameters using a novel optimization algorithm: Equilibrium optimizer", Superlattices Microstruct **146** (2020) 106665. https://doi.org/10.1016/j.spmi.2020.106665.

[65] A. Tasdelen & B. Sen, "A hybrid CNN-LSTM model for pre-miRNA classification", Sci Rep **11** (2021) 14125. https://doi.org/10.1038/s41598-021-93656-0.

[66] O. Baitiche, F. Bendelala, A. Cheknane, A. Rabehi & E. Comini, "Numerical modeling of hybrid solar/thermal conversion efficiency enhanced by metamaterial light scattering for Ultrathin PbS QDs-STPV cell", Crystals (Basel) **14** (2024) 668. https://doi.org/10.3390/cryst14070668.

[67] B. P. Babu & S. J. Narayanan, "One-vs-All Convolutional Neural Networks for synthetic aperture radar target recognition", Cybernetics and Information Technologies **22** (2022) 179. https://doi.org/10.2478/cait-2022-0035.

[68] A. Ziane, A. Rabehi, A. Rouabhia, M. Amrani, A. Douara, R. Dabou, A. Necaibia, M. Mostefaoui & N. Sahouane, "Numerical Investigation of G–V Measurements of metal – A Nitride GaAs junction", Revista Mexicana de Física **70** (2024) 061604. https://doi.org/10.31349/RevMexFis.70.061604.

[69] H. Helal, Z. Benamara, M. Ben Arbia, A. Khettou, A. Rabehi, A. H. Kacha, M. Amrani, "A study of current-voltage and capacitance-voltage characteristics of Au/n-GaAs and Au/GaN/n-GaAs Schottky diodes in wide temperature range", International Journal of Numerical Modelling: Electronic Networks Devices and Fields **33** (2020) e2714. https://doi.org/10.1002/jnm.2714.

[70] M. Guermoui, J. Boland & A. Rabehi, "On the use of BRL model for daily and hourly solar radiation components assessment in a semi-arid climate", The European Physical Journal Plus 135 (2020) 214. https://doi.org/10.1140/epjp/s13360-019-00085-0.

[71] A. Rabehi, A. Rabehi & M. Guermoui, "Evaluation of Different Models for Global Solar Radiation Components Assessment", Applied Solar Energy **57** (2021) 81. https://doi.org/10.3103/S0003701X21010060.

[72] M. Guermoui, A. Rabehi, K. Gairaa & S. Benkaciali, "Support vector regression methodology for estimating global solar radiation in Algeria", The European Physical Journal Plus **133** (2018) 22. https://doi.org/10.1140/epjp/i2018-11845-y.